Article:
Jegede, OE, Haque, N, Mullis, AM orcid.org/0000-0002-5215-9959 et al. (1 more author) (2021) Relationship between cooling rate and SDAS in liquid phase separated metastable Cu–Co alloys. Journal of Alloys and Compounds, 883. 160823. ISSN 0925-8388

https://doi.org/10.1016/j.jallcom.2021.160823

Relationship between cooling rate and SDAS in liquid phase separated metastable Cu - Co alloys.

Oluwatoyin E. Jegede [a], Nafisul Haque [a,I], Andrew M. Mullis [a] and Robert F. Cochrane [a]*

[a] School of Chemical & Process Engineering, University of Leeds, Leeds LS2 9JT, UK.

[I] Department of Metallurgical Engineering, NEDUET, Karachi, Pakistan

Email: pmoej@leeds.ac.uk , engrnafis@neduet.edu.pk, A.M.Mullis@leeds.ac.uk, R.F.Cochrane@leeds.ac.uk,

ORCID ID: https://orcid.org/0000-0001-6403-0637

https://orcid.org/0000-0002-0271-9209

https://orcid.org/0000-0002-5215-9959

https://orcid.org/0000-0001-5812-5226

Abstract

Cu-50 at. % Co and Cu-68.5 at. % Co metastable monotectic Cu-Co alloys have been rapidly solidified in a 6.5 m drop tube facility under nitrogen atmosphere. Microstructural evidences proved that liquid phase separation occurred in the alloys as predicted by the phase diagram of the alloy system. As well as liquid phase separated structures, substantial amount of dendrites were also observed. The resulting undercooled metal powders were sieved into ten size fraction range and the SDAS measurements taken using SEM images. Owing to the large number of liquid phase separated structures in the Cu-50 at. % Co alloy, SDAS measurements were taken from six size fractions while in the Cu-68.5 at. % Co alloy measurements were limited to three size range due to the fragmented nature of its dendrites as the droplet size fraction reduced. A regression relationship between cooling rate and the experimental SDAS measurements was established and an expression of the type $\lambda_{SDAS} = \Lambda(\dot{T})^{-n}$ was observed in both of the alloys in which the exponential value (n) is approximately 0.2.

Keywords: Metastable alloys

Monotectic

Cooling rate

SDAS

Liquid phase separation

*Address correspondence to Email: pmoej@leeds.ac.uk and jegedeoluwatoyin@yahoo.com

1 Introduction

There is a number of rapid solidification methods of achieving undercooling in an alloy but the drop tube processing (DTP) method of containerless processing has the added advantage of rapid cooling with containerless state thereby limiting contamination and aiding achievement of deeper level of undercooling due to the elimination of likely heterogeneous nucleants in the melt [1]. Figure 1 is the calculated metastable phase diagram of the Cu-Co system showing the solidification path of two alloys of interest [2], it is expected when the Cu-Co alloy is sufficiently undercooled into the metastable miscibility gap (MG) which is a region under the equilibrium liquidus; liquid phase separation (LPS) occurs [2–5]. The LPS could either be by nucleation or spinodal decomposition.

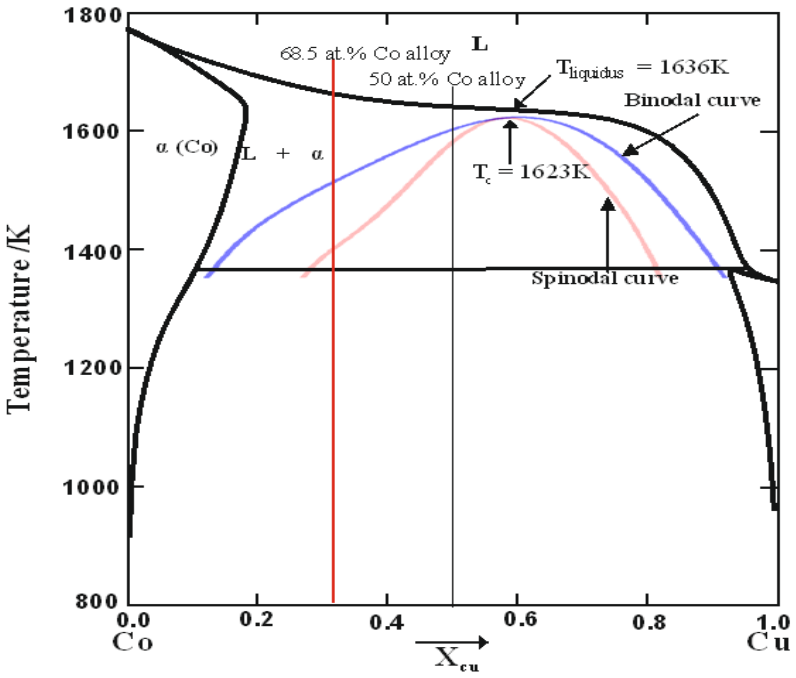

Figure 1: Metastable phase diagram of the Cu-Co system with calculated miscibility gap. The outer curve is the binodal curve while the inner one is the spinodal curve [2]**.**

The degree of undercooling attained has been said to be largely influenced by the cooling rate [4,6–9] and this in turn determines the type of microstructure formed. Higher cooling rates have been reported to have effect on Marangoni velocity induced as a result of the thermal gradient within a falling droplet which in turn has been said to accelerate the formation of core shell microstructures [2,10,11]. Liquid phase separated structures evidenced by presence of uniformly dispersed particles [2,7,8]; dendritic structures [2,4,6] as well as dual structures [2] (dendritic and liquid phase separated ones) have all been reported in undercooled Cu-Co alloys under the influence of various cooling rates. Fragmented dendrites have also been reported in Cu-Co alloys [2] as well as in other undercooled alloys [12,13].

Complexities of the DTP makes it difficult to experimentally measure the cooling rate [14] hence, theoretical model has been used in estimating it from the balance of the heat flux within the free falling droplet as a function of the droplet diameter taking cognisance of the thermo physical properties of the alloy being processed, latent heat from the droplet and convection heat transfer from the tube's atmosphere.

In short drop tubes such as used in this study, the cooling rate as a function of droplet size is determined using the following equation [15]:

$$\dot{T} = \frac{6}{\rho_m C_{pm} D}\left[h_d(T_D - T_R) + \varepsilon\sigma_{SB}\left(T_D^4 - T_R^4\right)\right] \qquad (1)$$

Where ρ_m and C_{pm} is the density and specific heat capacity of the alloy melt. D is the droplet diameter, T_D and T_R is droplet temperature during free fall and room/ ambient temperature respectively, ε is the total surface emissivity and σ_{SB} is the Stefan – Boltzmann's constant.

The heat transfer coefficient ,h_d, of the droplet falling through the gas is deduced from the Nusselt number (N_u) [16] using:

$$h_d = \frac{N_u \lambda_{gas}}{D} \quad (2)$$

N_u is dimensionless and combines the characteristic properties of the environment gas by the expression

$$N_u = 2.0 + 0.6 R_e^{1/2} Pr^{1/3} \quad (3)$$

Where Reynolds number (R_e) = $\frac{U_{term} \rho_{gas} D}{v_{gas}}$, (4) and Prandtl number (Pr) = $\frac{C_{pgas} v_{gas}}{\rho_{gas} \lambda_{gas}}$, (5), properties of the gas used are v_{gas}which is the kinematic viscosity, λ_{gas} is thermal conductivity, ρ_{gas} is density, C_{pgas} is specific heat and U_{term} is the terminal velocity which is the differential velocity between the droplet particle and gas. For a spherical droplet in a drop tube, U_{term} is given by the expression:

$$U_{term} = \sqrt{\frac{4gD}{3C_d}\left(\frac{\rho_L - \rho_{gas}}{\rho_{gas}}\right)} \quad (6)$$

Where ρ_L is the density of the liquid melt, g is acceleration due to gravity and C_d is the coefficient of drag exerted on the falling droplet. C_d is dependent on the Reynolds number and is determined from Stokes' flow by the expression

$$C_d Re^2 = \frac{4mg}{\Pi \rho_{gas} v_{gas}^2} \quad (7)$$

Where m is the mass of the droplet.

The heat transfer coefficient is then determined using equations (8)

$$h_d = \frac{\lambda_{gas}}{D}\left(2 + 0.6\sqrt{Re}\sqrt[3]{Pr}\right) \quad (8)$$

The estimated cooling rates by the method above vary considerably in magnitude. Jegede et al. [2] quoted values ranging from 10^2 to 10^4 Ks^{-1} for both the Cu-50 at. % Co and Cu-68.5 at. % Co alloys. These values are lower by one order of magnitude to that quoted by Kolbe and Gao [8] for the alloy system. A number of reasons could be responsible for the variance in the cooling rates of the Cu-Co alloy. It could be due to the composition of the alloy as observed in [2] and [8] which is totally explainable by the asymmetric nature of the MG curve as there is tendency for decrease of cooling rate with increased cobalt content. Also, environment of the drop tube is crucial as helium environment would have better thermal conductivity than a nitrogen atmosphere.

It is also possible to estimate the cooling rate from experimental data by taking measurements of the secondary dendrite arm spacing (SDAS). During the solidification process, dendrite coarsening occurs when dendrites with fine branches re-melt into the solidifying melt and thick branches continue to grow; the final SDAS is therefore largely determined by this coarsening process [17,18]. Researchers therefore proposed that the SDAS is better related to the solidification rate since it is formed during this coarsening process and therefore is a better measure of the cooling rate during solidification [17–21].

In 8 m drop tube processed binary Al-Cu alloys; Kasperovich et al. [22] observed that at cooling rates of 155 – 14,070 Ks^{-1}, SDAS decreased with increasing cooling rates with smaller droplets having the least SDAS. Also, in binary Cu-Sn droplets, Yi et al.[23] observed that SDAS was restrained in smaller droplets which are characterised by higher cooling rates. Various studies also reported similar findings of strong dependence of the SDAS on the cooling rate [19,24–28]. Most of the studies found that the larger the SDAS, the higher the amount of solute due to longer diffusion distances in

the melt. This observation is reasonable as at higher SDAS values, the cooling rate and undercooling is lower and therefore longer time to attain equilibrium; this explains the maximum non – equilibrium structures observed in [22]. SDAS refinement has also been said to occur with increased cooling rate [27]. This is believed to be as a result of increased undercooling resulting in more nucleation. With favoured nucleation and growth, concentration varies along the secondary dendrite arms and the resultant effect of this is heightened diffusion rate thereby impeding coarsening of dendritic arms and favouring formation of more needle-like dendrites. Overall volume fraction of dendrites has also been shown to decrease with increased cooling rates [27].

Based on the coarsening of the dendrite arms, a well-known practical expression relating SDAS to the cooling rate ($\dot{T}$) has been given by the equation [17]:

$$\lambda_{SDAS} = \Lambda(\dot{T})^{-n} \quad (9)$$

Where λ_{SDAS} is the secondary dendrite arm spacing (μm), Λ is a material dependent constant (μm $(Ks^{-1})^{n}$) [29] and the dimensionless exponential term (n) is said to be between 0.33 and 0.50 [17].

Various values for the constant (Λ) and the exponential term (n) have been reported in literature for different alloys and even alloys within the same alloying system [25]. It is however interesting that there has been no mention of these parameters for the Cu-Co alloy system. This might not be unconnected to the metastable LPS the alloy is susceptible to when rapidly solidified.

Literature suggested that due to the re-melting of the fine dendrites, there is heightened tendency for the parameters to vary as the concentration of the liquid phase changes [18,30,31] and Eskin et al. [25] found in the Al-Cu binary alloy system that (Λ) was

composition sensitive as it decreases with increasing amounts of copper. The exponential term also varied but was found to be rather less sensitive [25]. Horwath and Mondolfo [19] also observed in the alloy system that the SDAS varied with changing composition of the solidifying liquid. These observations are in line with the findings that the driving force for dendrite coarsening is the concentration gradient enacting from the varying surface energies of different sized dendritic arms [29]. A model similar to equation (9) proposed by Feurer and Wunderlin [20] and Kirkwood [18] considered the enrichment of the melt by the dissolving fine dendritic arms; with the initial liquid composition varying considerably with temperature as the solidification process proceeds and eventually getting to the composition C_1, which is the composition of the final liquid to solidify [18]. The value of the exponential term in their equation was 0.33. Their formulae relating SDAS to cooling rate can be written as:

$$\lambda_{SDAS} = K\left(M\dot{T}\right)^{-1/3} \tag{10}$$

With the constant M (m^3s^{-1}) [32] approximated by

$$M = -\frac{\Gamma D_{liq} \ln\left(C_1/C_0\right)}{m_L(1-k_0)(C_1-C_0)} \tag{11}$$

Where the numerical constant, K, is 5.5 [20] or 5.0 [18], Γ is the Gibbs – Thomson coefficient, D_{liq} is the diffusion coefficient of the solute in the liquid, C_0 is the overall alloy composition, m_L is the liquidus slope and K_0 is the partition coefficient.

Equation (10) is of particular interest in the study of SDAS in metastable Cu-Co alloys as with increased cooling rates, the degree of undercooling increases and the propensity for LPS especially in smaller droplets is favoured. According to the phase diagram of

the system, the composition of the demixed liquids is constantly adjusting during the course of the solidification process.

Although it is assumed that undercooled droplets of liquid phase separated metastable alloys cannot be dendritic in nature, literature established the possibility of dendritic formations in such droplets. This research work therefore seeks to contribute to the body of knowledge on dendritic formations in liquid phase separated metastable Cu-Co alloys and provide novel insights into the correlation between SDAS and cooling rate in demixed Cu-Co alloys.

2 Experimental methods

A detailed description of the production of the alloys considered in this article and their full metallographic preparation is available in an earlier publication [2]. The sieved metal powders were hot mounted in transoptic resin and prepped for microstructural analysis. In order to have better contrast between the regions in the droplets, etching was done with Nital solution (2% nitric acid and 98% propan-2-ol) and this preferentially dissolved the Co- rich phase. Imaging was subsequently taken using a Carl Zeiss Evo MA15 SEM in backscatter mode.

Although five variations of the linear intercept method of measuring SDAS from micrographs were described by Vandersluis and Ravindran in their publication comparing measurement methods for SDAS [33], two of such methods were attempted in this research. In figure 2, the measurement is taken by measuring the centreline to centreline distance between the dendrite arms (method E in the cited work) while in figure 3; the SDAS is determined by taking the length of the dendrite trunk and dividing

it by the number of visible arms (method D). The average SDAS values form both methods were similar but the second method with lower mean error of 0.04 was found to be consistently accurate and was adopted.

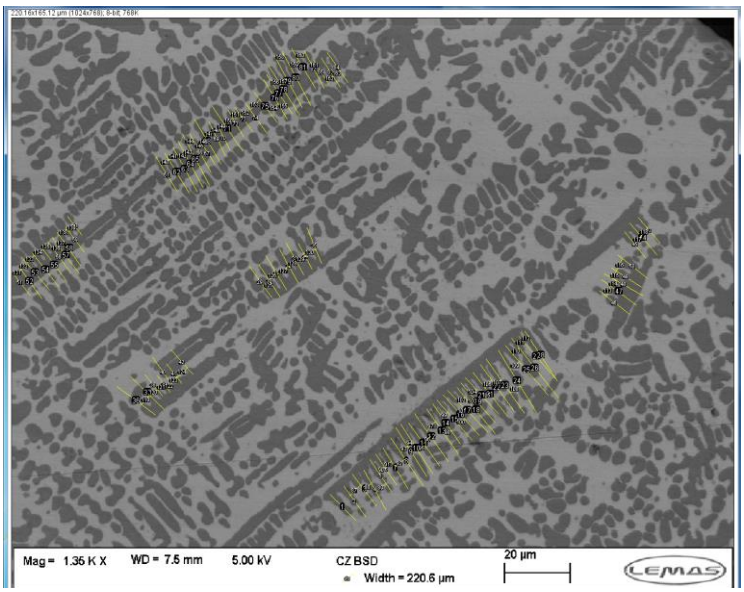

Figure 2: Measurements of SDAS in the Cu – 50 at. % Co alloy done by measuring the mid-point of adjacent dendrite arms.

Figure 3: Measurements of SDAS in the Cu – 68.5 at. % Co alloy done by measuring the length of the dendrite trunk and dividing by the number of visible arms.

3 Results and Discussion

3.1 Microstructural variations

Drop tube powders of both alloys were observed to have liquid phase separated and non-liquid phase separated structures. The liquid phase separated structures comprise of stable and evolving core shell structures (figures 4 and 5a respectively) as well as dispersed spherical particles (figure 5b). The non-liquid phase separated structures are dendrites some of which were observed to be fragmented. Simultaneous dendritic and liquid phase separated characteristic features were also observed in some droplets. Figure 5c is one of such droplet in which clear dendritic and liquid phase separated features can be observed. The dendritic structures are the focus of this research.

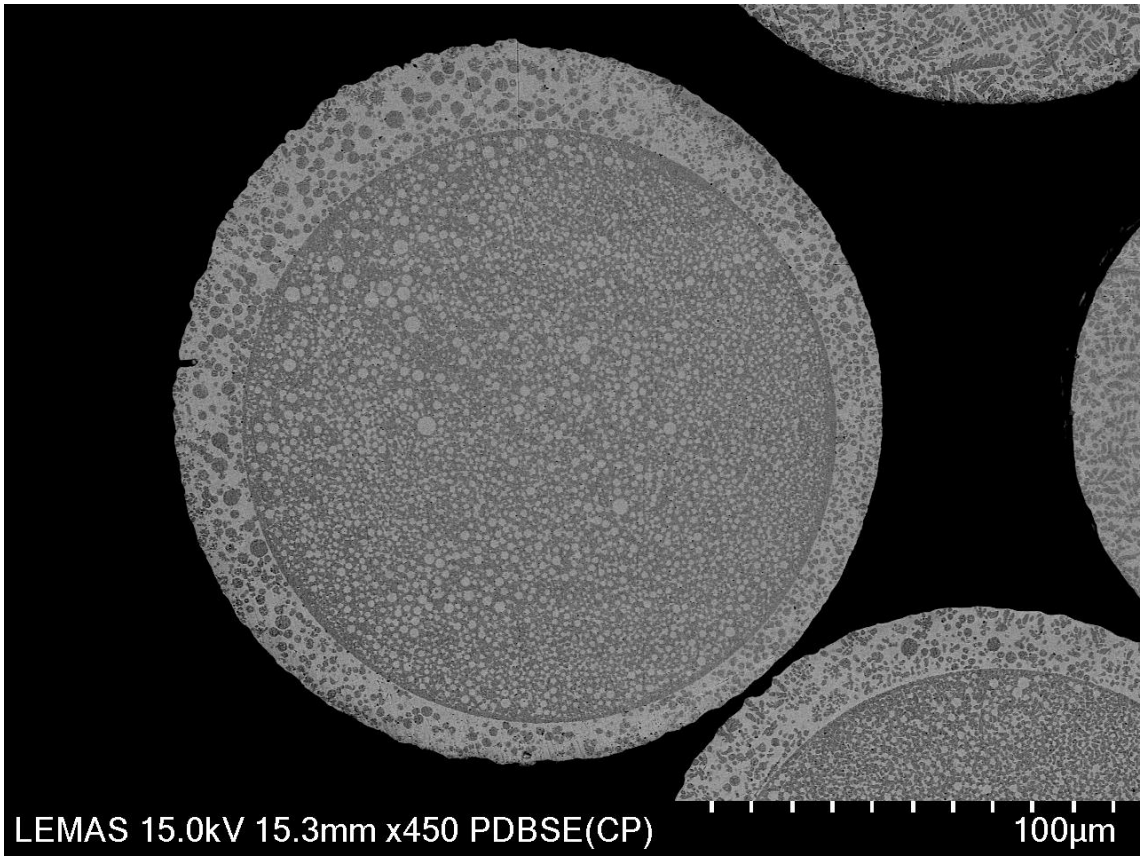

Figure 4: Fully evolved stable core shell structure in undercooled Cu – Co alloy showing cobalt rich core (dark region) and copper rich shell (lighter outer region).

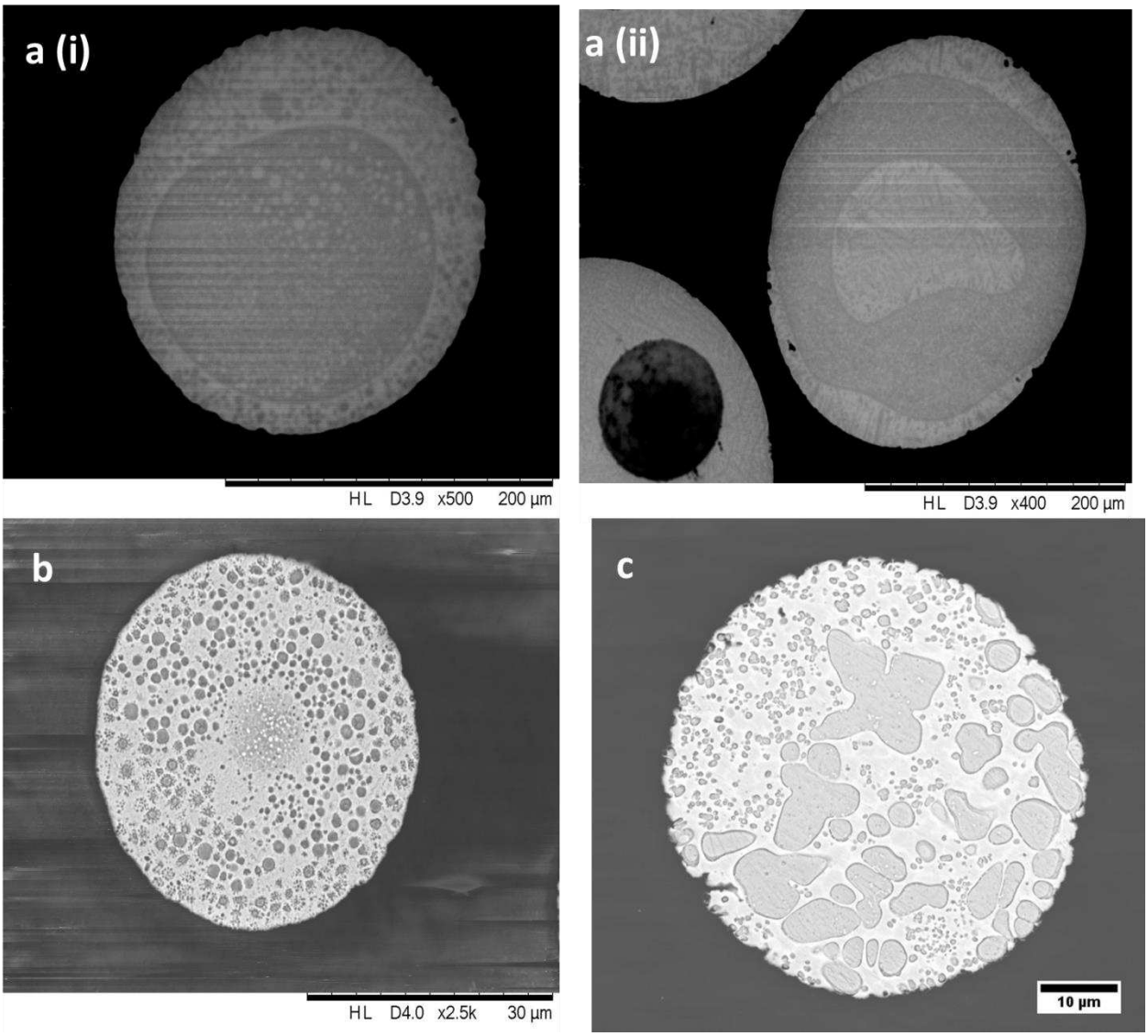

Figure 5: Liquid phase separated structures in drop tube processed Cu-Co alloys, (a (i) and (ii)) evolving core shell structures at different stages, (b) droplet with dispersed spherical particles and (c) mixed droplet showing dendritic features and dispersed spherical particles. Dark particles are Co – rich, lighter particles are Cu-rich.

In the Cu-50 at. % Co alloy, six size fractions were found to have droplets with dendrites having well defined arm spacing (figure 6a) while in the Cu-68.5 at. % Co alloy only three size fractions were found adequate (see table 1) as smaller sieve fractions in this alloy were found to contain fragmented dendrites as seen in figure 6b.

Table 1: Lower sieve size range of droplets with dendrites having well-defined arm spacing in drop tube processed Cu - Co alloys.

Alloy	Lower sieve size range (μm)					
Cu-50 at. % Co	850	500	300	212	150	106
Cu-68.5 at. % Co	850		500		300	

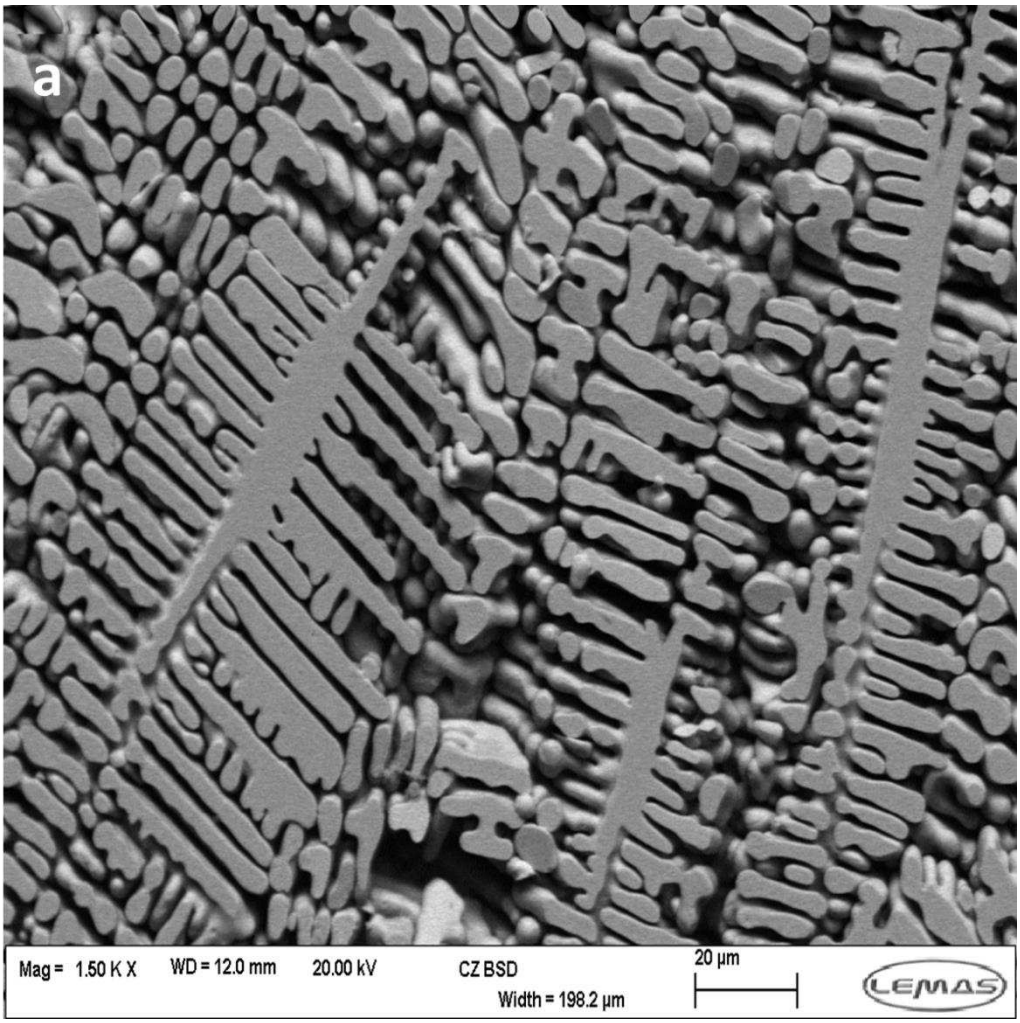

Figure 6a: Dendritic droplet from the Cu-50 at. % Co alloy showing dendrite with well – defined arm spacing (etched 5 minutes).

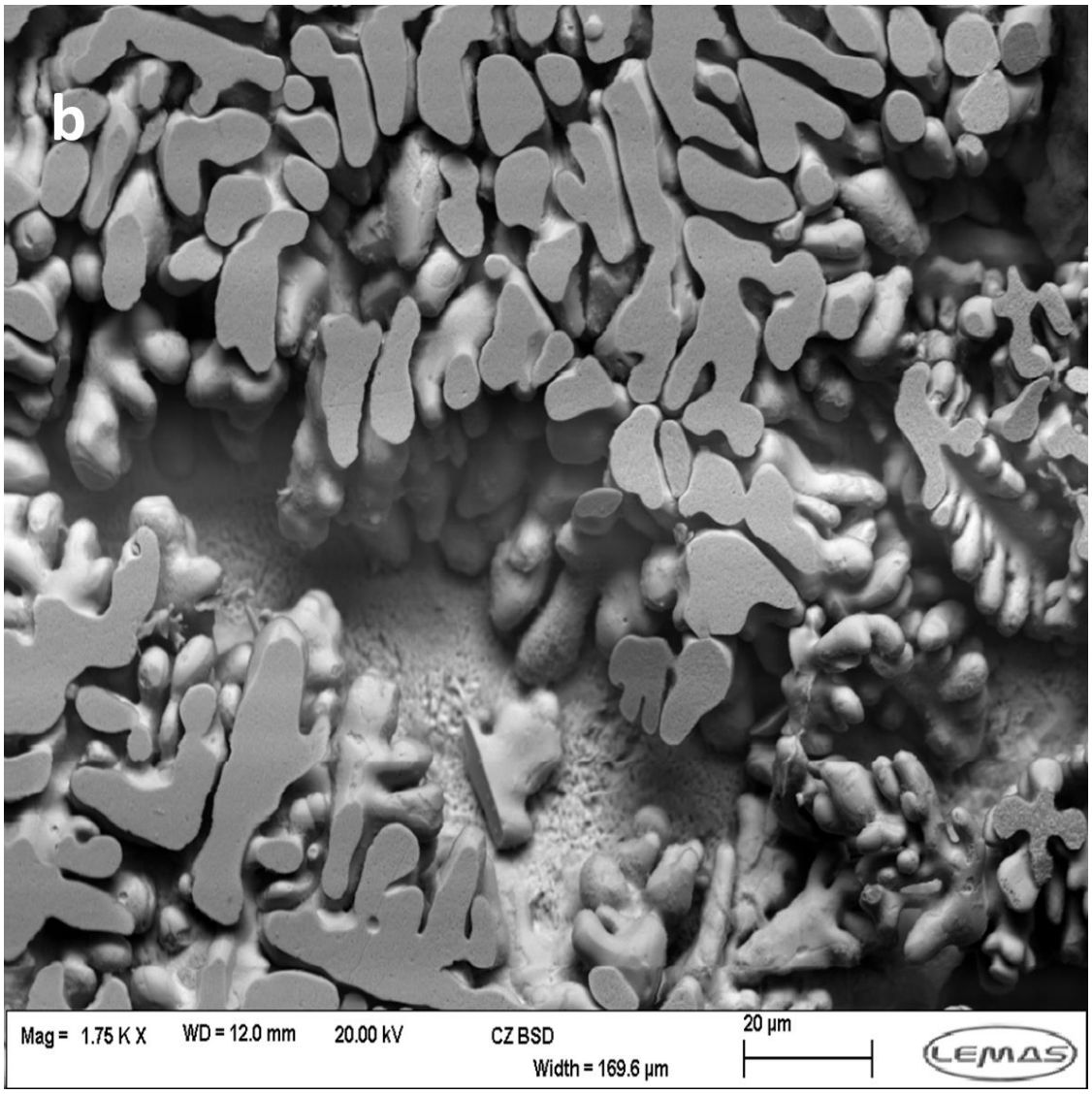

Figure 6b: Dendritic microstructures in drop tube processed Cu – Co alloys showing fragmented dendrites in deeply etched (10 minutes) droplet from the Cu-68.5 at. % Co alloy.

3.2 Droplet size effect on cooling rate

The plot of the cooling rate as a function of droplet diameter (after equation 1) is shown for both alloys in figure 7; values for the individual alloys are close hence are almost indistinguishable on the scale. Thermo physical properties for the processing gas and Cu-Co melt used for the calculation are listed in table 2. The estimates may be

approximated by the fitted power function of (1.687 x 10^7) (d/μm)$^{-1.469}$ for the Cu-68.5 at. % Co alloy and (1.815 x 10^7) (d/μm)$^{-1.476}$ for the Cu-50 at. % Co alloy.

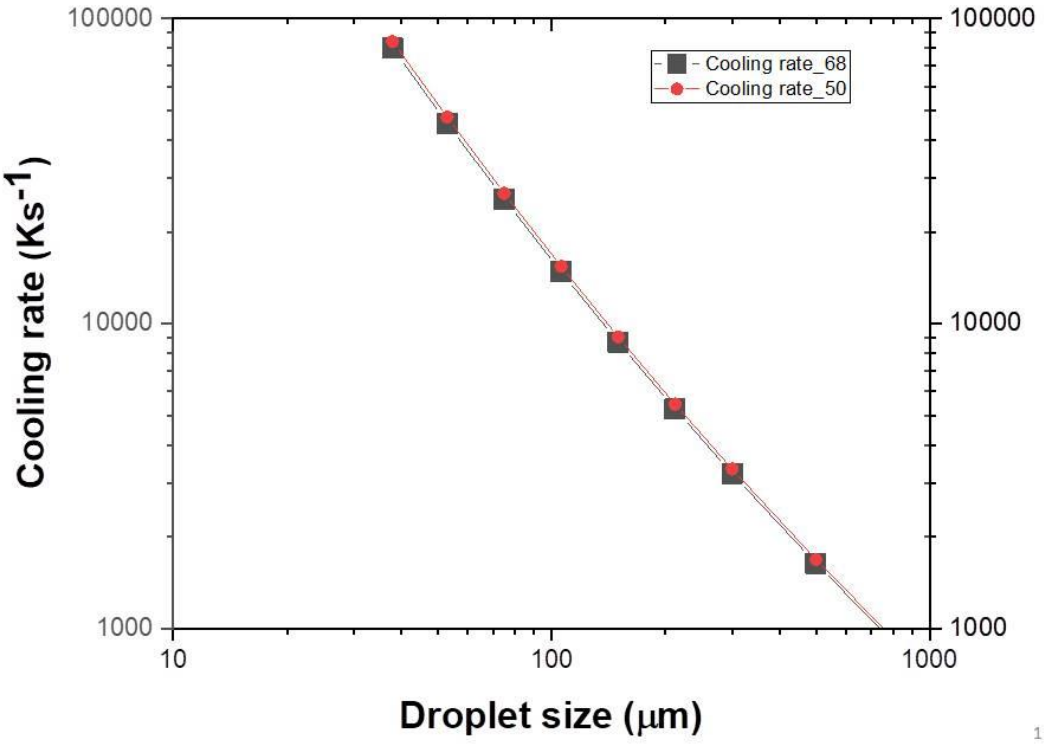

Figure 7: Calculated cooling rate as a function of droplet diameter in liquid phase separated Cu-Co alloys.

Table 2: Thermophysical properties of gas and Cu-Co melts.

Parameter	Unit	Value
Specific heat capacity (Cg)	J Kg^{-1} K^{-1}	1039
Thermal conductivity (λg)	W m^{-1} K^{-1}	2.4 X 10^{-2}
Dynamic viscosity (μg)	N s m^{-2}	1.76 X 10^{-5}
Prandt number (Pr)		0.7619
Specific heat capacity (C_m)	J Kg^{-1} K^{-1}	590 [a](50% Co)
Specific heat capacity (C_m)	J Kg^{-1} K^{-1}	627 [a](68.5% Co)
Density of melt (ρ_m)	Kg m^{-3}	7885 [a](50% Co)
Density of melt (ρ_m)	,Kg m^{-3}	7835 [a](68.5% Co)
Latent heat of melting (L)	J Kg^{-1}	0
Emissivity of melt (ε)		0.3007 [a]
Stefan Boltzmann constant (σ_B)	W m^{-2} K^{-4}	5.67 X 10^{-8}

[a]Calculated from pure elements according to their atomic fractions.

The estimated cooling rate (using equation 1) for a 300 μm droplet in the Cu-50 at. % Co alloy is 3.3 x 10^3 Ks^{-1}, 9.0 x 10^3 Ks^{-1} for a 150 μm droplet and 2.7 x 10^4 Ks^{-1} for a 75 μm droplet. The corresponding values for the Cu-68.5 at. % Co alloy are 3.2 x 10^3 Ks^{-1}, 8.7 x 10^3 Ks^{-1} and 2.6 x 10^4 Ks^{-1} for the (300, 150 and 75) μm droplets respectively. These estimates are in tandem with figure 7 which shows increase of the cooling rate as the droplet size decreased. The implication of this on the solidification microstructure is that the smaller droplets with higher cooling rates are likely to undergo

metastable liquid phase separation (as seen in figure 8 which shows microstructure abundance with droplet size). Reason for this is that the higher the cooling rate, the greater the degree of undercooling and the likelihood of the alloy accessing the metastable miscibility gap and undergoing liquid phase separation. Also, cooling rates in the Cu-50 at. % Co alloy are slightly higher than that of the Cu-68.5 at. % Co alloy hence, the prevalence of more LPS structures in the Cu-50 at. % Co alloy. This is expected as phase diagram estimates for undercooling to initiate liquid phase separation in the Cu-68.5 at. % Co alloy is slightly higher. Prevalence of fragmented dendrites compared to dendrites with visible arms was also observed as the cooling rate increases as shown in figure 9. The reason for the fragmentation of the dendrites is not known. Herlach et al. [12] in their paper postulated this is connected to the process of structure refinement which is known to occur during the solidification of undercooled melts at higher undercooling. However, Behulova et al. [13] in their work on rapidly solidified alloy powder stated that fragmented dendrites show the onset of the process of microstructure transition from dendritic to non – dendritic structures. The isolated fragments are said to move within the solidifying droplet and possibly change shape and size during the process. The claims of Behulova et al. [13] cannot be verified in this experiment but we did observe some droplets with perfectly aligned spherical and non – spherical dispersed particles (see figure 10). If indeed the process described by Behulova et al. [13] were to occur in metastable monotectic Cu-Co alloys that have undergone liquid phase separation as ours, the possible explanation would be that under the influence of weak fluid flow, the fragmented dendrites of varying composition are re – melted back in to the bulk melt. Upon further cooling into the miscibility gap, LPS

occurs in this remnant bulk liquid and this would explain the dual dendritic and liquid phase separated structure shown in figure 5c.

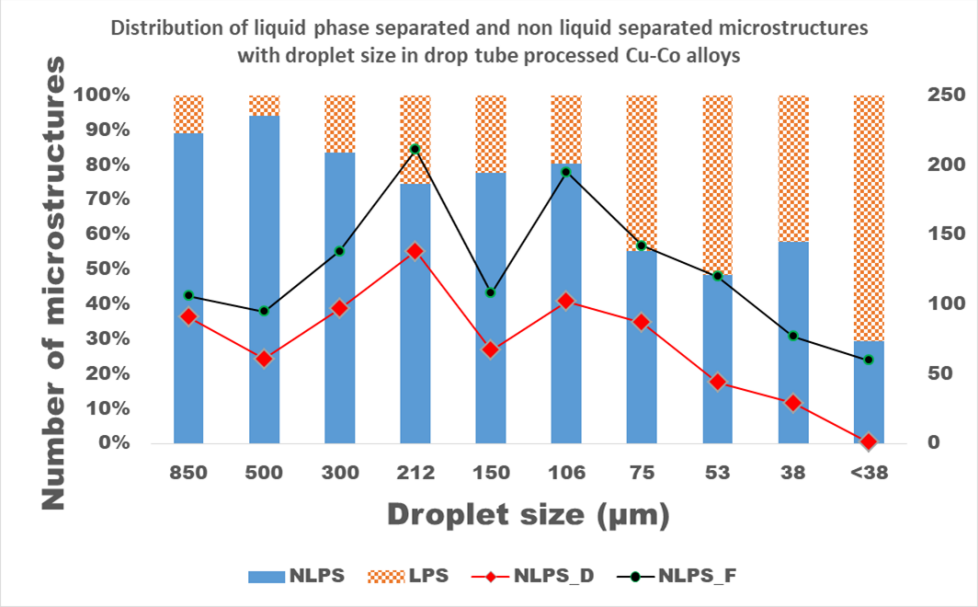

Figure 8: Microstructural variation of liquid phase separated (LPS), non – liquid phase separated (NLPS), non – liquid phase separated dendritic (NLPS_D) and non – liquid phase separated fragmented dendrite (NLPS_F) structures with droplet size in drop tube processed Cu-Co alloys.

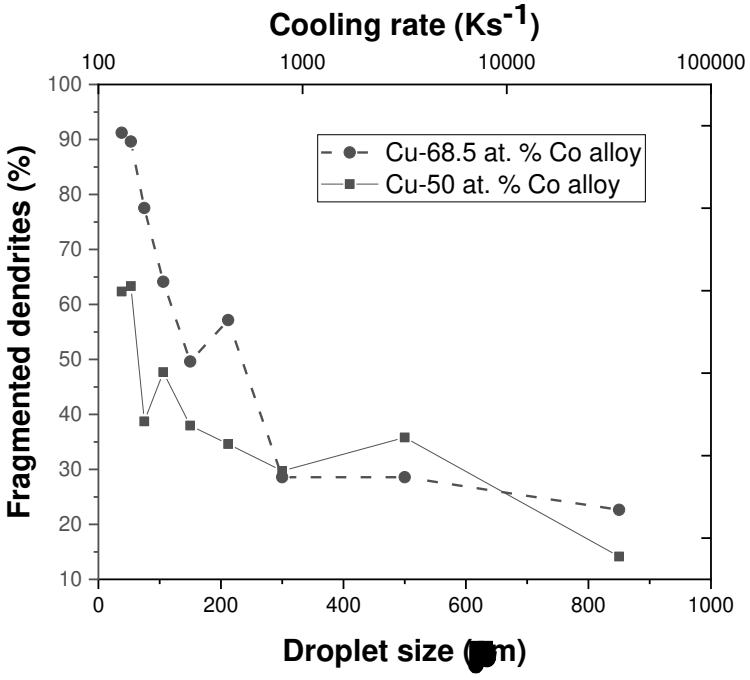

Figure 9: Prevalence of fragmented dendrites with droplet size in Cu-Co alloys.

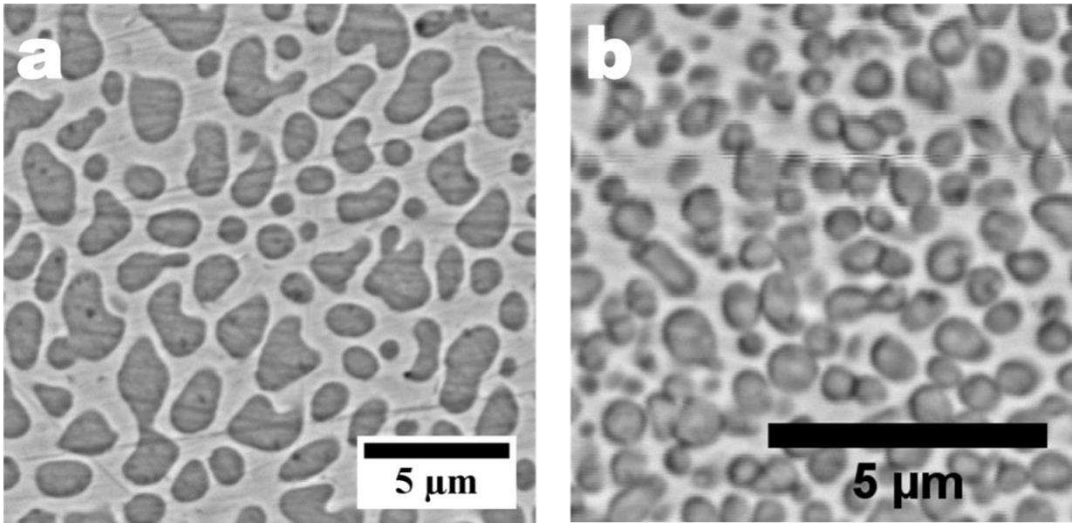

Figure 10: Dispersed (a) non – spherical and (b) spherical particles in liquid phase separated Cu-Co alloys.

3.3 SDAS

The frequency distribution of the observedSDAS per sieve size fraction in each alloy was plotted; figure 11 is an example of such plot which shows the frequency distribution of SDAS in two sieve size fractions of the two alloys. The standard deviation was computed from the distribution and the error bars representing $\pm$ 1 of the standard deviation shows the spread around the mean of the measured SDAS (figures 12a and b). Although the error bars indicate high variability in the data, the calculated coefficient of variation (which is the standard deviation divided by the mean) in both alloys are < 1. Error bars on the Cu-50 at. % Co alloy are lower than in the other alloy because more data points were available for analysis in this alloy (explained in section 3.1).

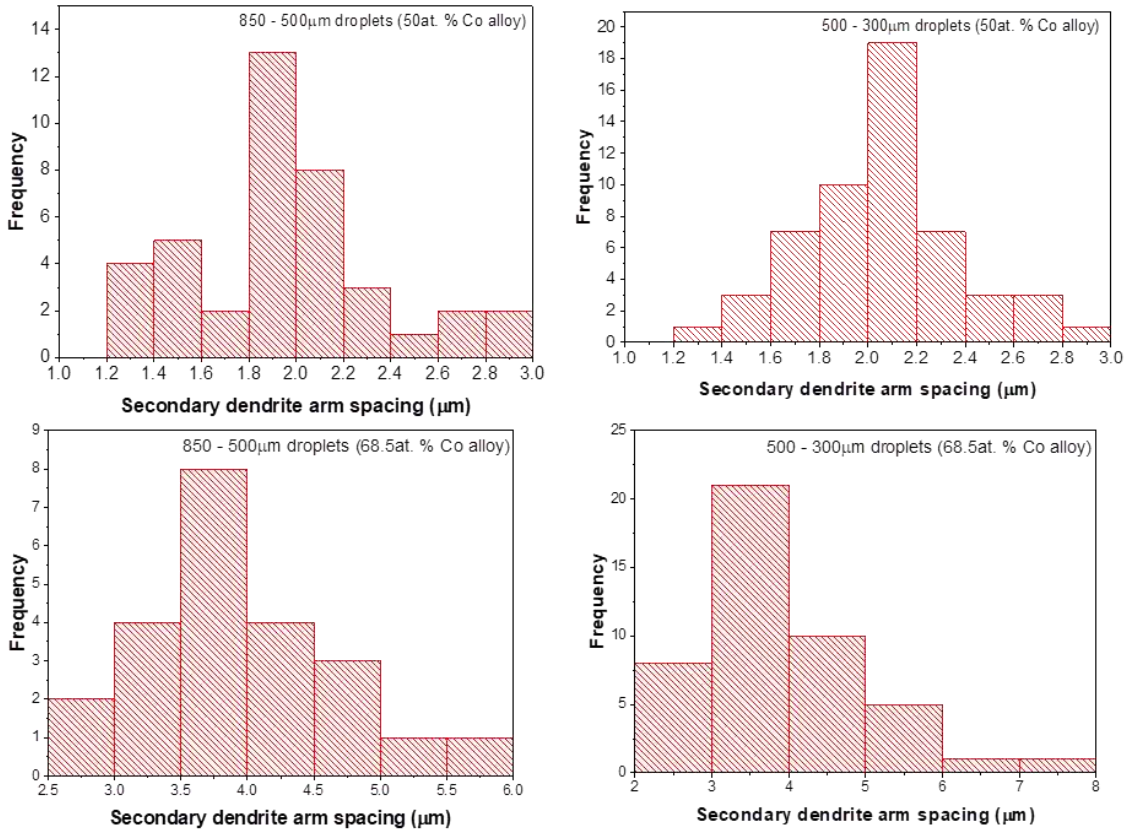

Figure 11: Frequency distribution of SDAS in 850 – 500 μm and 500 – 300 μm sieve size range of the Cu – 50 at. % and Cu-68.5 at. % Co alloys.

In figures 12a and b, the cooling rate is noticed to increase steadily as the droplet diameter decreased. It is also noticed that as the droplet size decreased, SDAS also decreased implying there exists a linear relationship between the SDAS and cooling rate. The implication of this is that smaller droplets with higher cooling rates have lower SDAS values which is totally expected as such droplets would have high undercooling and in a metastable alloy like the Cu-Co, liquid phase separation and fragmentation of dendrites is more probable. The cooling rate and undercooling effect also explains the occurrence of higher SDAS values in the Cu-68.5 at. % Co alloy than in the other alloy with higher estimated cooling rates. Observations in this research are in line with literature finding regarding the SDAS and the cooling rate [19,22,24,27] as well as with

the conclusions of [31] that SDAS decreases with increasing concentration of copper. This tendency with copper variation in the Cu-Co alloy system is totally explainable by the phase diagram of the alloy. As the copper concentration of the alloy increases, the probability of undercooling into the miscibility gap becomes higher and so also is the likelihood of liquid phase separation. As explained in Jegede et al. [2], The Cu-50 at. % Co alloy requires lesser undercooling than the Cu-68.5 at. % Co alloy in order to access the miscibility gap. The implication of this based on the assumptions of [13] is that alloys with high copper content like the Cu-50 at. % Co alloy are likely to experience faster dendrite fragmentation thereby restraining dendritic growth and resulting in more refined morphology than a lower copper content alloy. This would explain the lower SDAS values measured in the alloy compared to the Cu-68.5 at. % Co alloy which also has the higher dendritic fraction.

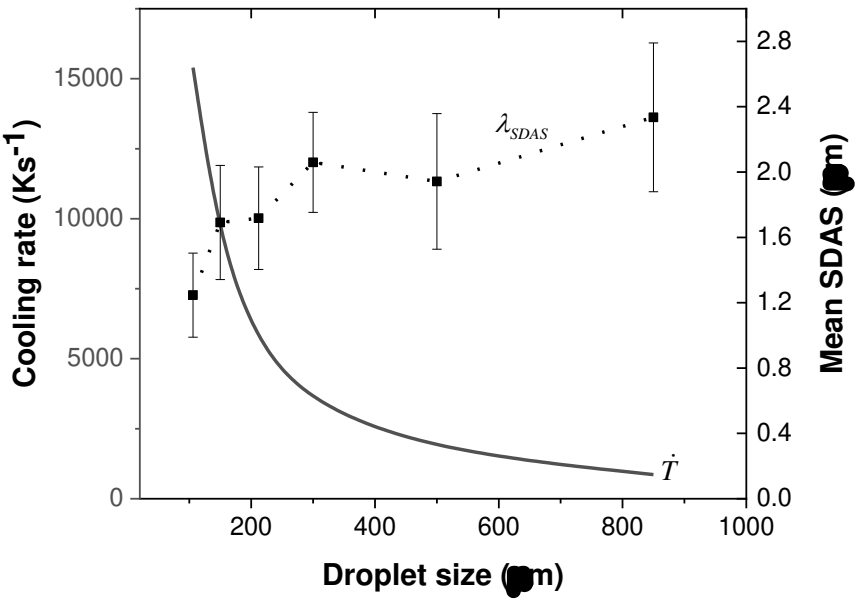

Figure 12a: SDAS(λ_{SDAS})variation with cooling rate($\dot{T}$) for different diameter of Cu-Co drop tube powders of composition 50 at. % Co.

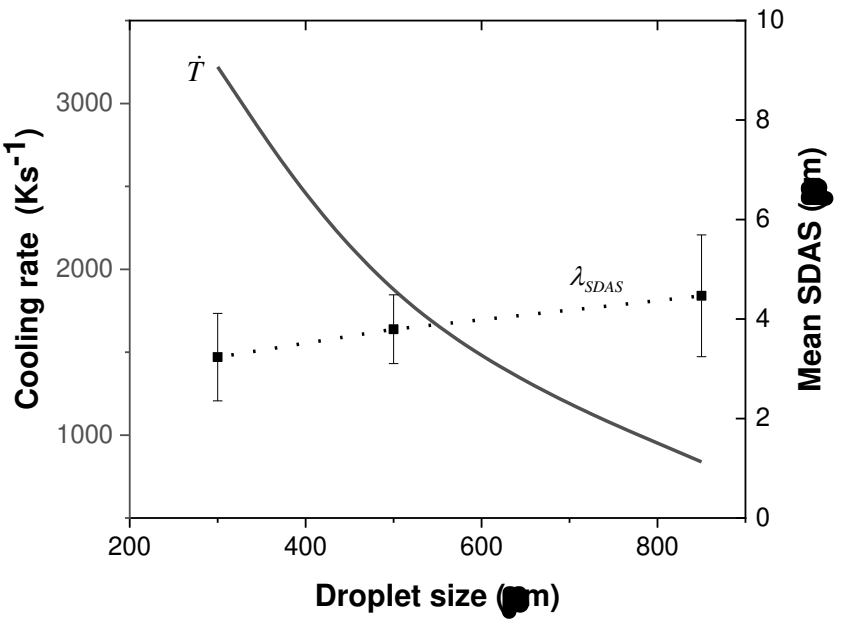

Figure 12b: SDAS (λ_{SDAS})variation with cooling rate($\dot{T}$) for different diameter of Cu-Co drop tube powders of composition 68.5 at. % Co.

In order to establish the existence of the linear relationship after equation (9) in the alloy system, a log – log plot of the mean SDAS per size is plotted against the estimated cooling rate per size (see figure 13). The constants of the relationship are derived by carrying out regression analysis of the plots. The result shows equation of the type $\log \lambda_{SDAS} = \log A + B \log(\dot{T})$ exists in the Cu-68.5 at. % Co alloy and solving this gave the following expressions denoting the relationship between the cooling rate and SDAS in the Cu-68.5 at. % Co alloyas:

$$\lambda_{SDAS} = 22.41(\dot{T})^{-0.239} \quad (12)$$

The linear analysis of the log – log plot of the Cu-50 at. % Co alloy returned a low R – square value of 0.83 and linear equation given in (13) below:

$$\lambda_{SDAS} = 8.23(\dot{T})^{-0.184} \quad (13)$$

Kasperovich et al. [22] postulated in their article that at low cooling rates in the presence of convective flow, there is the possibility of the deviation of the SDAS dependence on cooling rate from cube root to square root law. A number of fitting options were therefore attempted for this alloy but the linear fit returned the best R – square value which is quite reasonable based on earlier observations in figures 11a and b, suggesting the existence of some sort of linear relationship between the cooling rate and SDAS in the alloy system.

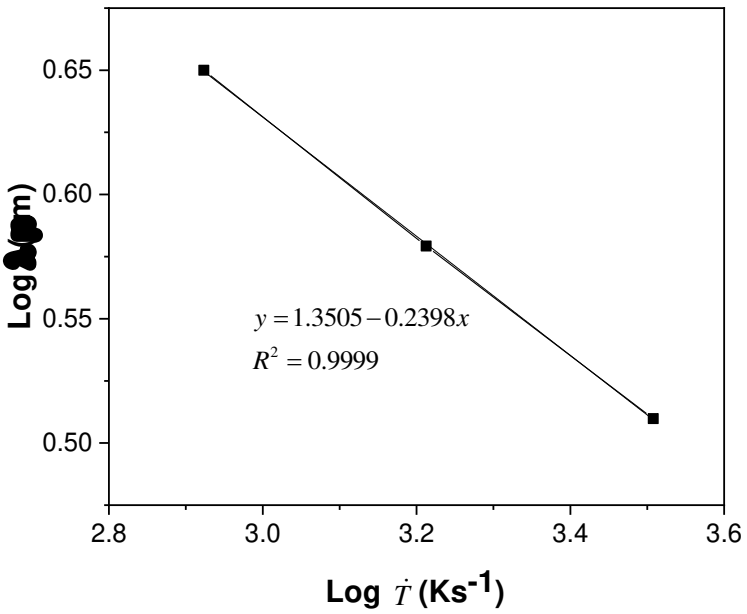

Figure 13: relationship between log (Ṫ) and log λ_{SDAS} in the Cu-68.5 at. % Co alloy.

The exponential term (n) has been said to show mild sensitivity to copper composition [25] but is relatively stable for an alloy system and this has been established by equations (12) and (13) that irrespective of the composition of the Cu-Co alloy system, n, is approximately 0.2 which is in line with the findings that value of ,n, is constant for increasing concentration of copper in Al – Cu binary alloys [25]. Although, the

observed value of the exponential term in this research is outside the range cited in most literature (between 0.3 and 0.5), this is thought to be as a result of the liquid phase separation that occurred in the Cu-Co alloys. As the alloys solidifies, heightened undercooling results in liquid phase separation leading to the formation of core shell microstructures as well as dendrites and other liquid phase separated structures. The compositions of the separated Cu – and Co – rich liquid phases from which the dendrites are growing is constantly adjusting but the overall composition of the droplet is constant hence the value of the exponential term obtained.

Equations (12) and (13) also showed that the value of the constant, λ, in the 50 at. % Co alloy is lower compared to the other alloy. This result collaborates the finding that the value of the material constant, λ, varies with the concentration of copper [25,31]. Probable explanation for this is that asides from having more copper content, this alloy is more prone to LPS and formation of core shell microstructure than the 68.5 at. % Co alloy. The formation of these core shell microstructures is characterised by the continuous enrichment of the centre of the parent droplet with Co – rich particles thereby depleting the periphery of the droplet (shell) of cobalt and making it Cu – rich. Observations of the dendritic structures in this experiment showed preference for growth in sectors of the droplet that are Cu – rich. Image 14 is an example showing dendritic structure in Cu – rich section of a Co – rich core.

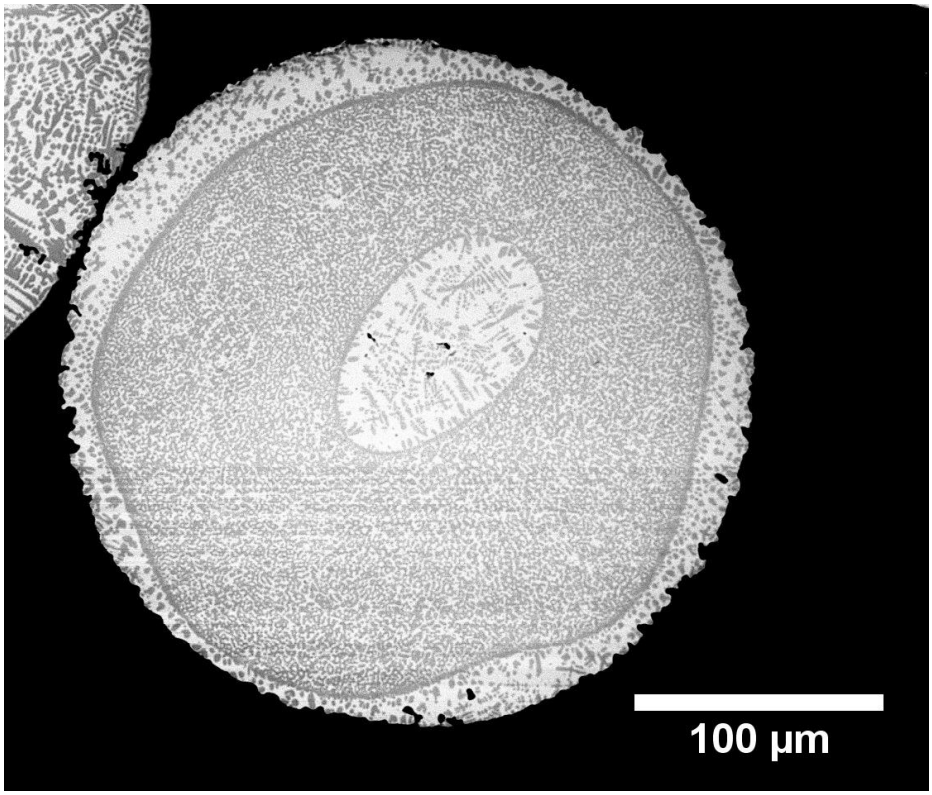

Figure 14: Dendrites in Cu – rich section of Co – rich core of an evolving core shell structure in the Cu-50 at. % Co alloy.

As there are no literature available for reference as at the time this article was written, it is not sure if this is applicable to Cu-Co alloys processed via other methods or if the values are constant for the alloy system.

4 Conclusion

It has been established that substantial dendritic formations as well as liquid phase separated structures are possible in Cu – Co alloys that are undercooled into the miscibility gap. It has been deduced that in drop tube processing estimation of the cooling rate from heat balance within the droplets vary considerably.The SDAS measured directly in drop tube alloys is a more reliable measure of explaining

microstructural variations.A regression relationship between the SDAS and cooling rate is established and validated in drop tube processed Cu – Co alloys.The exponential term in the regression equation for the Cu – Co alloy system is lower than most quoted values but deduced to be fairly constant for the alloy while the material constant variable was found to be sensitive to the concentration of copper in the alloys.

Acknowledgements: Oluwatoyin Jegede is a commonwealth scholar, sponsored by the UK government.

Conflict of interest: The authors declare they have no conflict of interest related to this work.

References

[1] D.M. Herlach, Containerless undercooling and solidification of pure metals, Annu. Rev. Mater. Sci. 21 (1991) 23–44.

[2] O.E. Jegede, R.F. Cochrane, A.M. Mullis, Metastable monotectic phase separation in Co–Cu alloys, J. Mater. Sci. 53 (2018) 11749–11764.

[3] A. Munitz, R. Abbaschian, Two-melt separation in supercooled Cu-Co alloys solidifying in a drop-tube, J. Mater. Sci. 26 (1991) 6458–6466.

[4] A. Munitz, R. Abbaschian, Microstructure of Cu-Co Alloys Solidified at Various Supercoolings, Metall. Mater. Trans. A. 27 (1996) 4049–4059.

[5] I. Yamauchi, N. and Ueno, M. and Shimaoka, I. and Ohnaka, Undercooling in Co – Cu alloys and its effect on solidification structure, J. Mater. Sci. 33 (1998) 371–378.

[6] C. Cao, N. Wang, B. Wei, Containerless rapid solidification of undercooled Cu-Co peritectic alloys, Sci. China Ser. A Math. 43 (2000) 1318–1326.

[7] X.Y. Lu, C.D. Cao, M. Kolbe, B. Wei, D.M. Herlach, Microstructure analysis of Co-Cu alloys undercooled prior to solidification, Mater. Sci. Eng. A. 375–377 (2004).

[8] M. Kolbe, J.R. Gao, Liquid phase separation of Co-Cu alloys in the metastable miscibility gap, Mater. Sci. Eng. A. 413–414 (2005) 509–513.

[9] X. Luo, L. Chen, Investigation of microgravity effect on solidification of medium-low-melting-point alloy by drop tube experiment, Sci. China Ser. E Technol. Sci. 51 (2008) 1370–1379.

[10] R. Dai, S.G. Zhang, Y.B. Li, X. Guo, J.G. Li, Phase separation and formation of core-type microstructure of Al-65.5 mass% Bi immiscible alloys, J. Alloys Compd. 509 (2011) 2289–2293.

[11] C. Xu, R. Du, X.J. Wang, S. Hanada, H. Yamagata, W.H. Wang, C.L. Ma, Effect of cooling rate on morphology of primary particles in Al-Sc-Zr master alloy, Trans. Nonferrous Met. Soc. China (English Ed. 24 (2014) 2420–2426.

[12] D.M. Herlach, K. Eckler, A. Karma, M. Schwarz, Grain refinement through fragmentation of dendrites in undercooled melts, Mater. Sci. Eng. A. 304 (2001) 20–25.

[13] M. Behulova, R. Moravcik, M. Kusy, L. Caplovic, P. Grgac, L. Stancek, Influence of atomisation on solidification microstructures in the rapidly solidified powder of the Cr--Mo--V tool steel, Mater. Sci. Eng. A. 304 (2001).

[14] D.M. Herlach, D. Holland-Moritz, P. Galenko, Metastable solids from undercooled melts, Elsevier, 2006.

[15] J. Zarling, Heat and mass transfer from freely falling drops at low temperatures, NASA STI/Recon Tech. Rep. N. (1980).

[16] R.B. Bird, W.E. Stewart, E.N. Lightfoot, Transport phenomena, Wiley, New York, 1960.

[17] M.C. Flemings, Solidification Processing, Metall. Trans. 5 (1974) 2121--2134.

[18] D. Kirkwood, A simple model for dendrite arm coarsening during solidification, Mater. Sci. Eng. 73 (1985) L1–L4

[19] J. Horwath, L. Mondolfo, Dendritic growth, Acta Metall. 10 (1962) 1037–1042.

[20] U. Feurer, R. Wunderlin, DGM Fachber. 38 (1977) (Deutsche Gesellschaft für Metallkunde,Oberursel)., in W. Kurz and D.J. Fisher, Fundamentals of Solidification, Trans Tech Publications, Switzerland, (1986), Appendix 8.

[21] D. Bouchard, J.S. Kirkaldy, Prediction of dendrite arm spacings in unsteady-and steady-state heat flow of unidirectionally solidified binary alloys, Metall. Mater. Trans. B. 28 (1997) 651–663.

[22] G. Kasperovich, T. Volkmann, L. Ratke, D. Herlach, Microsegregation during solidification of an Al-Cu binary alloy at largely different cooling rates (0.01 to 20,000 K/s): modeling and experimental study, Metall. Mater. Trans. A. 39 (2008) 1183–1191.

[23] X. Yi, N. Ellendt, X. Li, V. Uhlenwinkel, U. Fritsching, Characterization of cooling rate and microstructure of CuSn melt droplet in drop on demand process, Trans. Nonferrous Met. Soc. China. 27 (2017) 1636–1644.

[24] N. Wang, B. Wei, Rapid solidification of undercooled Cu--Ge peritectic alloy, Acta Mater. 48 (2000) 1931–1938.

[25] D. Eskin, Q. Du, D. Ruvalcaba, L. Katgerman, Experimental study of structure formation in binary Al--Cu alloys at different cooling rates, Mater. Sci. Eng. A. 405 (2005) 1–10.

[26] A.M. Mullis, L. Farrell, R.F. Cochrane, N.J. Adkins, Estimation of cooling rates during close-coupled gas atomization using secondary dendrite arm spacing measurement, Metall. Mater. Trans. B Process Metall. Mater. Process. Sci. 44 (2013) 992–999.

[27] R. Chen, Y. Shi, Q. Xu, B. Liu, Effect of cooling rate on solidification parameters and microstructure of Al- 7Si- 0.3 Mg- 0.15 Fe alloy, Trans. Nonferrous Met. Soc. China. 24 (2014) 1645–1652.

[28] W. Zhang, L. Liu, X. Zhao, T. Huang, Z. Yu, M. Qu, H. Fu, Effect of cooling rates on dendrite spacings of directionally solidified DZ 125 alloy under high thermal gradient, Rare Met. 28 (2009) 663.

[29] J. Wiskel, K. Navel, H. Henein, E. Maire, Solidification study of aluminum alloys using impulse atomization: Part II. Effect of cooling rate on microstructure, Can. Metall. Q. 41 (2002) 193–204.

[30] V. Ronto, A. Roosz, The effect of the cooling rate or the local solidification time and composition on the secondary dendrite arm spacing during solidification PART II: Al—Mg—Si alloys, Int. J. Cast Met. Res. 14 (2001) 131–135.

[31] V. Ronto, A. Roosz, The effect of cooling rate and composition on the secondary dendrite arm spacing during solidification. Part I: Al-Cu-Si alloys, Int. J. Cast Met. Res. 13 (2001) 337–342.

[32] W.R. Osorio, A. Garcia, Modeling dendritic structure and mechanical properties of Zn--Al alloys as a function of solidification conditions, Mater. Sci. Eng. A.

325 (2002) 103–111.

[33] E. Vandersluis, C. Ravindran, Comparison of Measurement Methods for Secondary Dendrite Arm Spacing, Metallogr. Microstruct. Anal. 6 (2017) 89–94.